Nuclear Instruments and Methods in Physics Research B 315 (2013) 55–59

Contents lists available at SciVerse ScienceDirect

Nuclear Instruments and Methods in Physics Research B

journal homepage: www.elsevier.com/locate/nimb

Adsorption of S on the (1 1 1) surfaces of the noble metals Ag and Au studied by direct recoiling spectroscopy

Ezequiel Tosi, Gustavo Daniel Ruano, Silvina Bengió, Leonardo Salazar Alarcón, Esteban Alejandro Sánchez, Mohamed Khalid, Oscar Grizzi *, María Luz Martiarena, Guillermo Enrique Zampieri

Centro Atómico Bariloche-CNEA, Instituto Balseiro – UNCuyo, Instituto de Nanociencia y Nanotecnología, CNEA, CONICET, Avda. E. Bustillo 9500, R8402AGP S.C. de Bariloche, Río Negro, Argentina

ARTICLE INFO

Article history:
Received 12 October 2012
Received in revised form 22 March 2013
Accepted 15 April 2013
Available online 4 July 2013

Keywords:
Ion scattering spectroscopy
Direct recoil spectroscopy
Sulphur adsorption on noble metals

ABSTRACT

In this work we present a study of the adsorption of S on the surfaces of the noble metals Au(1 1 1) and Ag(1 1 1) by ion scattering performed in the forward direction. Low energy electron diffraction patterns taken at specific exposures were used to identify the S phases. Photoemission and Auger electron spectroscopies were used to determine the coverage dependence on dose. All the techniques indicate that the adsorption process is different in both surfaces since very low coverages. Analysis of the scattering peak intensity and shape provides evidence about the coexistence of Ag substrate atoms together with the S adsorbate in the top layer for all the coverages investigated. For Au we discard this effect for coverages up to ~0.3 ML and measure a small Au recoil peak coming from the top layer for the high coverage regime (~0.5 ML). At intermediate coverages the shape of the scattering spectra presents a strong dependence on azimuth that is attributed to S–S shadowing and consistent with the diffraction symmetry. The variations on azimuth are analyzed with a simple shadowing calculation that uses the crystallographic model proposed by Yu et al. (2007) [1].

1. Introduction

The adsorption of S on the (1 1 1) surfaces of the noble metals Au and Ag has received ample attention partly due to their applications in electronic devices, in nanotechnology, and also because they still represent a classic challenge in adsorption phenomena far from been completely solved. Ag and Au are FCC crystals with very similar lattice parameters ($a_{Au} = 0.4079$nm and $a_{Ag} = 0.4086$nm). In spite of these similarities the adsorption of S on these surfaces proceeds very differently. This is clearly evidenced by the different Low Energy Electron Diffraction (LEED) patterns that both surfaces develop at specific coverages, some of which are yet to be understood. Here we use an ion scattering technique that allows us to study the S adsorption on both surfaces since the first stages of the process and under the same experimental conditions, thus allowing a better discerning of the differences (and similarities). In the past, several experimental and theoretical methods have been applied besides LEED, among them: photoelectron spectroscopy (XPS), Normal-Incidence X-ray Standing Wavefield absorption (NIXSW), Medium Energy Ion Scattering (MEIS), electrochemistry techniques, tunnelling microscopy (STM) and density functional theory [1–9]. In the present work we propose and discuss the potential of ion scattering and direct recoiling spectroscopy (DRS) [10] to study these systems. DRS has a high top layer sensitivity that is useful to detect the substrate mass transport necessary to form sulphide layers or to generate adatoms, and when combined with Time Of Flight (TOF–DRS) methods the surface damage becomes negligible allowing to take many spectra at different geometries. The shape of the spectra is strongly dependent on the surface crystallography although interpretation of these features may require complex trajectory simulations. Due to its more local character and its ability to identify atomic species, DRS is a good complement to both LEED and STM. In this work we discuss the evolution of the TOF–DRS spectra as a function of coverage which was first characterized by XPS and LEED. We obtain information about the eventual migration of Ag and Au substrate atoms to the adsorbate layer for specific coverages and discuss a simple shadowing model to account for the main TOF–DRS features observed at intermediate coverages in Au.

2. Experimental details

The XPS experiments were carried out in a vacuum generator chamber equipped with a CLAM 100 spectrometer and an Mg/Al photon source. In this case the S doser was mounted on a prechamber and the XPS measurements carried out immediately after dosing. The TOF–DRS measurements were performed on another

* Corresponding author.
E-mail address: grizzi@cab.cnea.gov.ar (O. Grizzi).

0168-583X/$ - see front matter © 2013 Elsevier B.V. All rights reserved.
http://dx.doi.org/10.1016/j.nimb.2013.04.084

home-made UHV chamber with the S doser mounted *in situ*. AES measurements carried out on this chamber gave the same evolution of the S and substrate signals with dosing time than the XPS measurements, allowing us to calibrate the coverage at specific exposures in both chambers. The Au(1 1 1) and Ag(1 1 1) single crystals (from Mateck) were prepared by cycles of low energy Ar sputtering and annealing, and their cleanliness and surface order were characterized by TOF–DRS, AES and LEED. In TOF–DRS, the samples were bombarded by a pulsed beam of 4.2 keV Ar^+ ions at different incidence angles (indicated with respect to the surface plane). A time-of-flight analysis of the primary recoiled target atoms and of the quasi-single scattered projectile atoms was then performed by using a detector (channel electron multiplier) placed at the end of a time-of-flight drift tube set at 45° with respect to the incidence beam direction. At the scattered energies (keV range), both neutral and ion scattered particles are detected with similar sensitivity thus avoiding uncertainties due to electron exchange processes.

The S layers were prepared by exposing the surfaces to a S_2 flux provided by a solid state Pt/Ag/AgI/Ag_2S/Pt electrochemical cell [11]. The cell was operated with an applied potential of 170 mV at a temperature of 190 °C. The pressure remained below 1 or 2×10^{-9} Torr during dosing.

3. Results and discussion

Most of the previous studies on Ag or Au have been performed separately and it becomes difficult to compare the kinetics of adsorption on both surfaces. It is therefore interesting to compare the growth on both surfaces, more precisely the amount of S incorporated on each surface under the same dosing times and experimental conditions. Fig. 1 shows the dependence of S coverage versus S dose for Au and Ag as measured with XPS taking care of maintaining the same dosing conditions, i.e., the same experimental geometry, and the same temperature and voltage on the doser. The curves show the ratios between the intensities of the S2p peaks, corrected for the photoemission cross sections, and the Au4f or Ag3d peaks, corrected for the photoemission cross sections and the attenuation lengths expressed in units of the (1 1 1) interplanar distances. These ratios represent the surface coverages as long as the S atoms form a single layer on top of the substrates, what presumably occurs for Au in the whole range shown in the figure, but only in the initial stages in the case of the Ag substrate. Several measurements were performed in order to ensure the reproducibility of the experiments. We observe two important differences between the surfaces: (1) at the beginning of the adsorption the sticking coefficient of Ag is three times larger than that for Au, which is in agreement with the expected higher reactivity in Ag, and (2) for larger doses there is saturation of the S signals in Au at around 0.5 ML, while in Ag it continues growing at a high rate.

The evolution of the LEED patterns also differs since the beginning of the process with characteristics that have been discussed previously [1,3,6,7]. In Fig. 1 we reproduce the main patterns that we have measured because they will help later to identify the surface symmetry condition under which the TOF–DRS spectra were taken. For the clean Au we observe the pattern typical of the $22x\sqrt{3}$ reconstruction, which is completely lifted at 5 min dosing time. At this coverage no fractionary diffraction spots are observed. Above 20 min dose (~0.25 ML) we observe a diffuse 5×5 pattern that gets better defined around 30–40 min (~0.3 ML). At slightly larger dose the 5×5 pattern develops into a $\sqrt{3}x\sqrt{3}$ (not always well defined) that changes rapidly into another diffuse pattern without well-defined spots, which upon annealing to 180° C transforms into a sharp and very stable phase, usually called the complex Au phase.

In Ag two main patterns are identified, one identified as $\begin{pmatrix} 3.67 & 0.00 \\ 3.00 & 3.5 \end{pmatrix}$ [7] whose surface geometry is not yet unravelled. This pattern appears at early doses and remains up to a dose of about 60 min where the $\sqrt{7}x\sqrt{7}$ R19° appears clearly, without requiring annealing as in Au. This stable phase in Ag has been associated with the growth of an Ag_2S alloy that can extend for many layers according to recent MEIS measurements [8].

In the following we concentrate on the TOF–DRS measurements. Typical sets of TOF–DRS spectra taken at 20° of incidence angle are shown in Fig. 2 for both samples and for several dosing times. The azimuthal incident angle was chosen along the $[\bar{2}11]$

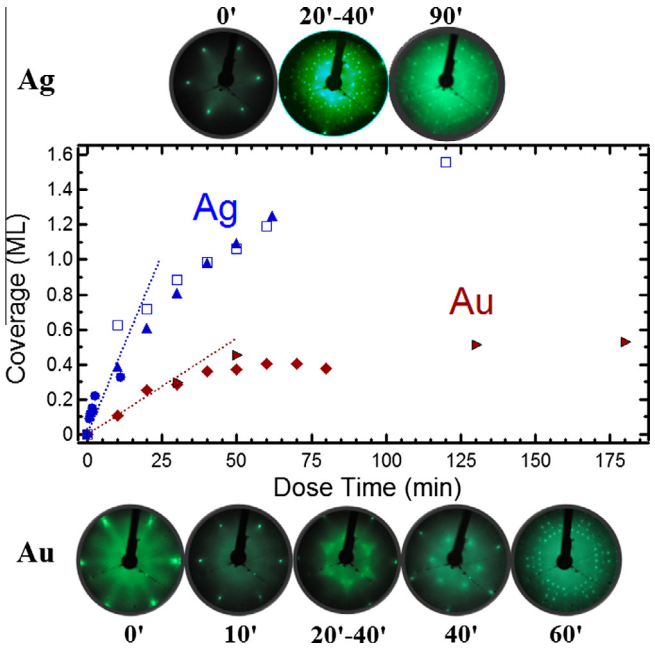

Fig. 1. Evolution of S coverage versus dosing time determined from XPS signals. Characteristic LEED patterns measured at the specified dosing times for the (1 1 1) surface of Au and Ag.

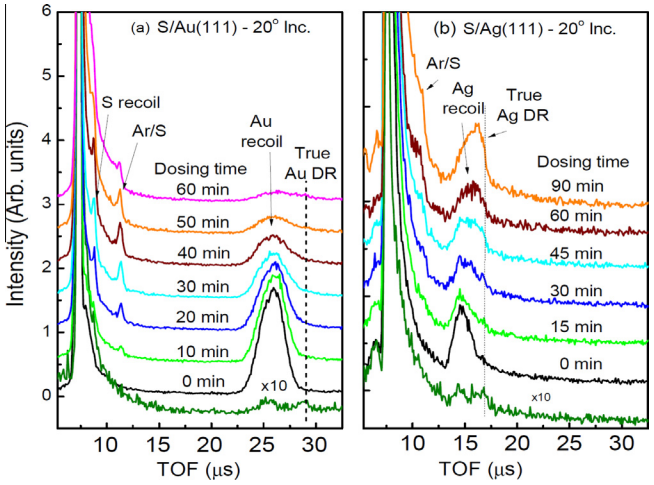

Fig. 2. TOF–DRS spectra measured with 4.2 keV Ar^+ along the $[\bar{2}11]$ azimuth from Au(1 1 1) (left) and from Ag(1 1 1) (right) for the clean surface (0 min) and for several S dosing times. The lowest spectrum in each plot was taken at grazing incidence (5°) to show up the position of true substrate DRs related to surface defects. The other spectra were taken at 20° incidence.

direction on both cases because it corresponds to the longest interatomic distance, the only one that allows detection of substrate recoils from the clean surface within our bombarding geometry and projectile energies [12]. The clean surface spectra (0 min) are comprised of mainly two peaks corresponding to Ar scattered from Ag or Au, and recoiled substrate atoms. The assignment of peaks is based on simple calculation of collision kinematics [10]. Because of the high surface atomic density, even along this azimuth, the substrate peaks appear shifted towards lower TOFs due to focusing and multiple collisions. A true substrate direct recoil (DR) is observed with very low intensity at grazing incidence and is attributed to surface defects or isolated atoms (bottom spectrum in each set of spectra of Fig. 2). At this angle a well-defined surface recoiling peak, coming from substrate atoms that go first to the surface and then are backscattered towards the detector [10,13] can also be observed at TOFs lower than the position corresponding to the true DR.

With increasing dosing times new features appear due to S recoils and Ar scattering off S. The increase of these new features is accompanied by a decrease in the substrate peaks due to shadowing by the adsorbates. Besides these common aspects, it becomes apparent that the behaviour of the adsorption process is different in both surfaces. In Au the S associated structures are "clean", narrow peaks as it could be expected for adsorbates without shadowing among them at this high incident angle (20°). For higher dosing times the S associated peaks stop increasing in height and become broader, more shoulder type. For Ag, the S associated structures are always broad since the very initial doses and are shoulder-like structures. The changes in the substrate peaks are also distinct. In Au the substrate recoil peak just decreases maintaining its position up to high dosing times. In Ag the Ag recoil peak decreases less than for Au even though the amount of S incorporated is higher for the same dosing time as confirmed by AES measurements after each adsorption step. Another difference is that the Ag recoil peak also shifts towards higher TOFs, i.e., towards the position of the true DR peak since the beginning of dosing.

The contrasting behaviour with dose is better evidenced in the difference spectra shown in Fig. 3. For Au the only significant components that appear positive (meaning that is higher in the spectrum at 20 min dose than for the clean surface spectrum) are the sharp S associated peaks. The strong negative Au recoil peak is due to the shadowing of the substrate by the S adlayer (seen as a decrease of this structure in Fig. 2). In contrast, the difference spectra of the Ag surface exhibit a more complex behavior. The S peaks are never as well defined as in Au, meaning that there are important shadowing effects since the beginning of the adsorption. The difference spectrum for 20 min dose shows a decrease of the intensity of the Ag recoil peak, characteristic of the clean surface, and an increase of the intensity at slightly higher TOFs, i.e., at the position of the true DR. The shift of this peak towards the position of the true DR means that after the S adsorption the top most Ag atoms are more visible for the Ar projectiles than in the clean surface. This same effect is seen even more pronounced in the difference spectrum after 90 min of dose, indicating that Ag atoms must be present in the top most layer at all S doses. At 90 min the general shape of the Au spectrum becomes more similar to the one for Ag, with the S peaks becoming broader. A difference that remains is that the Au recoil peak decreases even further (more negative in the difference spectrum). The behaviours described indicate for Au: (1) at low coverages, S is sitting above the last Au atomic layer without an appreciable amount of Au atoms at the top layer, (2) S atoms in Au are spread out at low coverages precluding strong shadowing effects at 20° incidence, (3) at high coverage, a reordering takes place in the surface that produces new shadowing effects that affect both the S peak shape and the background of the spectra. For Ag we observe that (1) S and Ag atoms coexist in the top layer since the first adsorption stages investigated, i.e., for both LEED patterns, and (2) they form structures that generate shadowing effects even at low coverages.

In the rest of the work we concentrate on some details of the adsorption of S on Au. In agreement with the observations in the literature [1–5], around 30 min of dosing time, corresponding to about 0.3 ML, there is a change in the surface order that is evidenced by the disappearance of the 5×5 LEED pattern and the changes in the shape of the TOF–DRS spectra discussed above. The high coverage structure is, at present, a subject of strong debate. Su Yin Quek et al. [3] proposed that this phase, obtained after annealing the S exposed surface to 180° C, correspond to a very stable AuS adlayer. This model implies an important transport of Au atoms to form a top layer with the same number of Au and S atoms. Another adsorption model described in the works by Pensa et al. [5] and by Lustemberg et al. [4], proposed the formation of S8 clusters and required less Au transport to the adlayer to interpret measurements carried out on samples prepared by immersion. Here, to obtain additional information about the Au transport to the adlayer, for example to determine at what stage of the adsorption process this Au transport begins, we measured spectra along other azimuthal directions as shown in Fig. 4. The left panel corresponds to spectra taken for 20 min dosing time along the $[\bar{2}11]$ and $[\bar{1}01]$ azimuths. The observation of an intense Au recoil peak along the $[\bar{2}11]$ azimuth and its complete absence along the $[\bar{1}01]$ azimuth

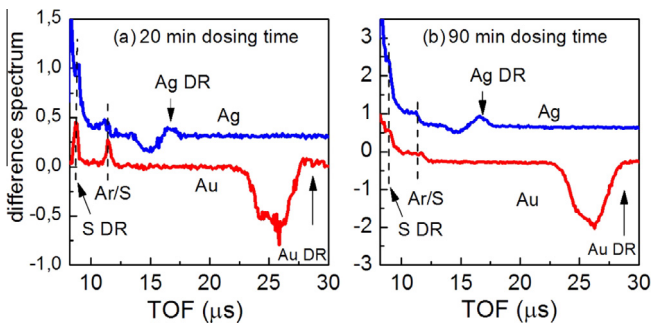

Fig. 3. Difference spectra obtained by subtraction of the spectrum measured at 20 min (left) and 90 min (right) dosing time and the corresponding clean surface spectrum.

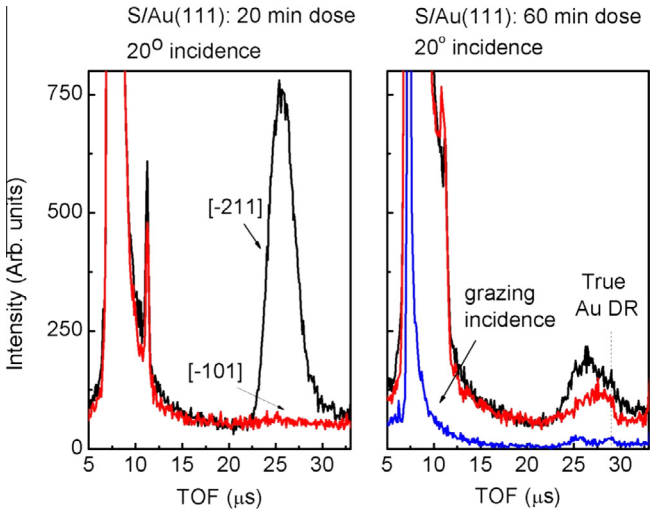

Fig. 4. Comparison of TOF–DRS spectra taken for Au along two different azimuths after 20 min (left) and after 60 min (right) of S dosing time.

is similar to what occurs in the clean surface. This suggests that at this coverage the substrate still keeps the clean surface crystallography without an appreciable amount of Au at the adsorbate layer. The right panel of Fig. 4 shows spectra taken at the same geometry but for the high coverage regime. Very interestingly, we observe that in spite of the increase in the S content now an Au recoil peak appears at the $[\bar{1}01]$ direction, where it was absent before, and that it is closer to the true DR position. This clearly indicates that some fraction of the Au substrate atoms have now moved up towards the adsorbed layer and are visible to the beam. The intensity of this Au recoil peak is of the order of 10% of the value measured along the $[\bar{2}11]$ azimuth for the clean surface, i.e., much smaller than the corresponding fraction observed in Ag, however, the existence of strong focussing effects in the clean surface precludes the use of the clean surface intensity for a quantitative determination. Annealing to 180° C did not produce a major change in the intensity of the Au recoil peaks along the studied directions, which means that before the annealing the atoms must be close to the positions corresponding to the complex phase but without the long range order required by LEED measurements. More measurements at backscattering conditions or with other projectiles may help to reduce the focussing effects and to determine which of the models proposed agree better with the experiment.

The final point we discuss is the dependence of the TOF–DRS spectra with azimuth for Au at low incident angles. We mentioned above that up to 40 min dose the S associated peaks in Au do not present shadowing effects at 20° incidence; however, at more grazing angles if the surface has a well-defined crystallography one should expect effects due to S–S shadowing and or focusing. In order to study these effects we measured spectra as a function of the azimuth using an incidence angle of 4°, and for a S coverage where the 5 × 5 LEED pattern starts to be observed. At this incident angle the S recoil peak presents a strong variation while the Ar contribution from the substrate remains weak; at incident angles larger than 5° this Ar contribution increases making the analysis of the S recoil more difficult. The corresponding spectra are shown in Fig. 5a; the azimuthal angle step between adjacent spectra is ~3.5°. The spectra show three peaks, the one at the left side is the Ar scattering involving substrate Au atoms, and the other two are due to S recoils and Ar scattering from S. The background changes due to multiple scattering processes and surface recoiling peaks that move in position depending on the substrate atomic positions along the specific azimuth [10,13]. The experimental values of the area of the S recoil peak are shown in Fig. 5b. The main source of error in the integration of the experimental S recoil peak area comes from the discrimination of the background and of the surface recoil structure (which appears as a broad contribution at the left of the recoil peak). Typically, the error in these estimations varies from 10% to 30%, i.e., much lower than the observed variations in Fig. 5b. A clear 60° symmetry is reproduced in both the general shape and the intensity of the spectra. This result is complementary to the information from the LEED patterns due to the more local character of TOF–DRS. In fact, the 5 × 5 LEED pattern is often seen superposed on a diffuse background (particularly at room temperature) that could indicate the presence of other structures without sufficient long range order to appear as clear diffraction spots. The high reproducibility of the TOF–DRS spectra every 60° indicate that if there are such local structures they also show the same symmetry.

A full description of the shape of the spectra and the changes with azimuth requires a detailed crystallographic model and complicated grazing trajectory calculations that are out of the scope of the present paper. Here we attempt a test of the model proposed in Ref. [1] and confirmed in recent LEED experiments [14] by using a

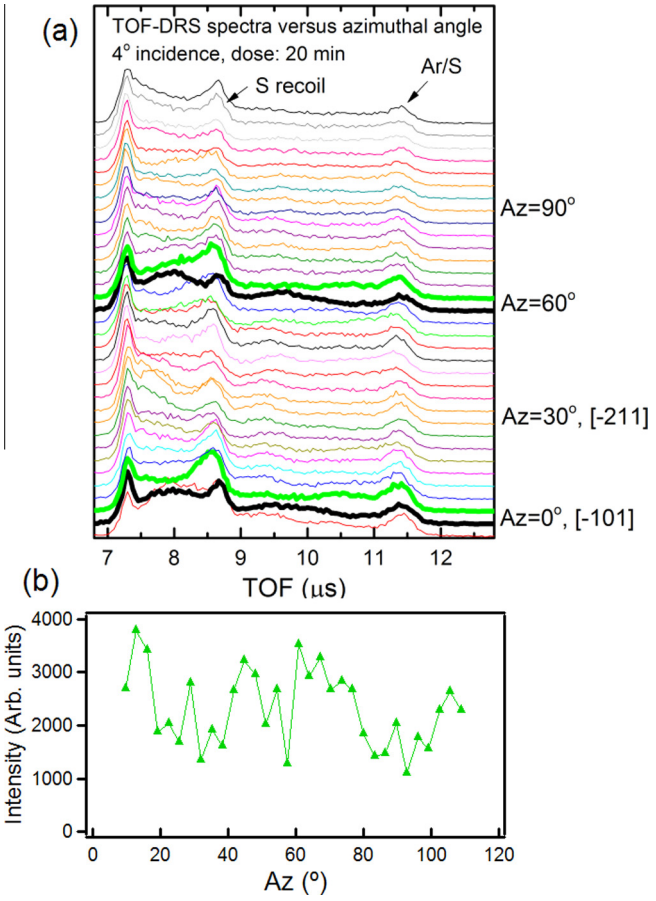

Fig. 5. (a) TOF spectra versus azimuth for the Au surface after 20 min S dosing time taken at 4° incidence. (b) Area of the S recoil peak versus azimuthal angle.

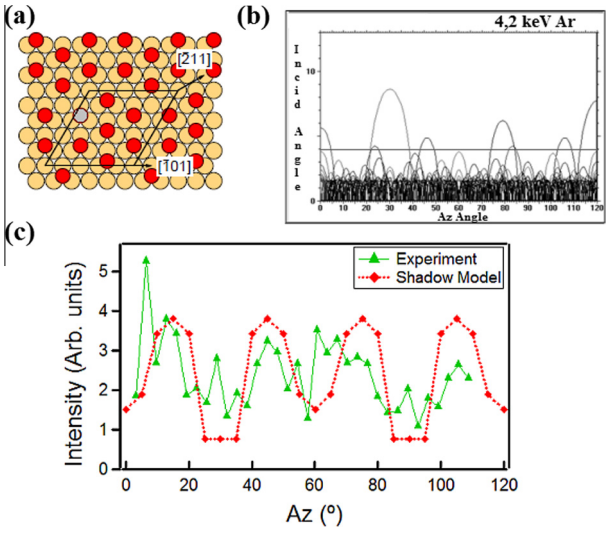

Fig. 6. (a) Schematics of the adsorption model proposed in Ref. [1]. (b) Shadow cone diagram for one of the seven S atoms in the cell unit (indicated in grey). (c) Estimation of the S contribution resulting from shadow cone calculations (azimuth 0 corresponds to the $[\bar{1}01]$ direction.

shadow cone calculation based on Moliere potentials [15]. The model proposed in Ref. [1] is shown in Fig. 6a. For the 5 × 5 unit cell of the model there is a cluster of seven S atoms. For each of the seven S atoms in the unit cell we calculated a shadowing

diagram as the one shown in Fig. 6b in incident and azimuthal coordinates for the S atom indicated in grey. At the 4° incidence used in the experiment (horizontal line in shadow cone diagram) some recoiling processes will be forbidden along specific azimuthal directions because of shadowing (for example along 30° azimuth where the 4° line goes into a shadowing region), and at other azimuths the recoiling process will be allowed (along 15° azimuth with the 4° line going above the shadowing region). When these simple considerations are accounted for the seven S atoms the variation of the S recoil contribution appears as the one plotted in Fig. 6c. We recall that it is necessary to include the contribution of the seven S atoms because for a specified ion direction each of the S atoms may follow a different shadowing process due to the different neighbouring atom positions. This calculation indicates that at all azimuths there are some S atoms in the cluster that are accessible to beam, i.e., the S intensity is never zero. We see that this simple model reproduces the main minima at 30° and 60°, the shallower minimum at 60° and approximately the position of the maxima, while other features are not accounted correctly. This qualitative agreement helps us to interpret the observed symmetry and would indicate at least some consistency between the crystallography proposed in Ref. [1] and the experimental observations of Fig. 5.

4. Summary

We studied the adsorption of S on Ag(1 1 1) and Au(1 1 1) under the same experimental conditions. Both XPS and AES showed a three times higher sticking coefficient on Ag than on Au. Since the beginning of the adsorption TOF–DRS spectra presented distinct features that support the coexistence of Ag and S atoms on the top layer for the two phases observed by LEED, and the lack of equivalent Au atoms in the adlayer up to intermediate coverages (0.3 ML). At high S coverages a fraction of Au recoils from the adlayer were detected that did not follow the clean surface crystallography. At intermediate coverages, an azimuthal study performed on Au revealed S–S shadowing effects that are consistent with the symmetry observed by LEED.

Acknowledgements

Fruitful discussions with Drs. H. Ascolani and J.E. Gayone are gratefully recognized. We acknowledge financial support from CONICET (PIP 112-200801-00958, 112-201101-00594, 112-201101-00650) and Universidad Nacional de Cuyo (06/383, 06/390, 06/332 and 06/C402).

References

[1] M. Yu, H. Ascolani, G. Zampieri, D.P. Woodruff, C.J. Satterley, R.G. Jones, V.R. Dhanak, J. Phys. Chem. C 111 (2007) 10904.
[2] J.A. Rodríguez, J. Dvorak, T. Jirsak, G. Liu, J. Hrbek, Y. Aray, C. González, J. Am. Chem. Soc. 125 (1) (2003) 276–285.
[3] M.M. Su Ying Quek, J. Biener, J. Biener, C.M. Bhattacharjee, U.V. Friend, E.J. Waghmare, J. Phys. Chem. B, Lett. 110 (2006) 15663;
M.M. Biener, J. Biener, C.M. Friend, Surf. Sci. 601 (2007) 1659.
[4] P.G. Lustemberg, C. Vericat, G.A. Benitez, M.E. Vela, N. Tognalli, A. Fainstein, M.L. Martiarena, R.C. Salvarezza, J. Phys. Chem. C 112 (2008) 11394.
[5] E. Pensa, E. Cortés, G. Corthey, P. Carro, C. Vericat, M.H. Fonticelli, G. Benitez, A.A. Rubert, R.C. Salvarezza, Acc. Chem. Res. 45 (8) (2012) 1183–1192.
[6] K. Schwaha, N.D. Spencer, R.M. Lambert, Surf. Sci. 81 (1979) 273.
[7] Yu. Miao, D.P. Woodruff, C.J. Satterley, R.G. Jones, V.R. Dhanak, J. Phys. Chem. C 111 (2007) 3152.
[8] A.J. Window, A. Hentz, D.C. Sheppard, G.S. Parkinson, D.P. Woodruff, T.C.Q. Noakes, P. Bailey, Surf. Sci. 604 (2010) 1254.
[9] S.C. Gómez-Carrillo, P.G. Bolcatto, Phys. Chem. Chem. Phys. Vol. 13 (2011) 461.
[10] J.W. Rabalais, Principles and Applications of Ion Scattering Spectrometry. Surface Chemical and Structural analysis, Wiley-Interscience, 2003.
[11] W. Heegemann, K.H. Meister, E. Bechtold, K. Hayek, Surf. Sci. 49 (1975) 161.
[12] Luis M. Rodríguez, J.E. Gayone, E.A. Sánchez, H. Ascolani, O. Grizzi, M. Sánchez, B. Blum, G. Benitez, R.C. Salvarezza, Surf. Sci. 600 (2006) 2305–2316.
[13] M. Shi, O. Grizzi, H. Bu, J.W. Rabalais, Phys. Rev. B 40 (1989) 10163.
[14] G.M. McGuirk, H. Shin, M. Caragiu, S. Ash, P.K. Bandyopadhyay, R.H. Prince, R.D. Diehl, Surf. Sci. 610 (2013) 42.
[15] J.E. Gayone, R.G. Pregliasco, E.A. Sánchez, Y.O. Grizzi., Phys. Rev. B. 56 (1997) 4186.